

# Effect of Blocking $I_{Kur}$ on the Genesis of Repolarisation Alternans in Canine Atrium

Na Zhao<sup>1</sup>, Qince Li<sup>1</sup>, Kuanquan Wang<sup>1</sup>, Runnan He<sup>1</sup>, Yongfeng Yuan<sup>1</sup>, Henggui Zhang<sup>1,2,3,4\*</sup>

<sup>1</sup>Harbin Institute of Technology, Harbin, China

<sup>2</sup>The University of Manchester, Manchester, UK

<sup>3</sup>SPACenter Space Science and Technology Institute, Shenzhen, China

<sup>4</sup>Pilot National Laboratory of Marine Science and Technology, Qingdao, China

## Abstract

*The Kv1.5 channel-mediated, ultra-rapid delayed rectifier  $K^+$  current ( $I_{Kur}$ ) is a promising target for anti-arrhythmic drugs due to its 'atrial-selective' property. However, whether blocking  $I_{Kur}$  induced action potential (AP) prolongation in normal atria can increase the alternans susceptibility has not yet been investigated.*

*This study aimed to investigate the effects of blocking  $I_{Kur}$  on the genesis of repolarisation alternans which is associated with arrhythmogenesis. The updated canine atrial cell model developed by Ramirez *et al.* was used to implement the dynamic pacing protocol and the standard S1-S2 protocol to obtain rate dependent curve and restitution curve to analyse the alternans.*

*Simulation results showed the prolonged AP and increased  $Ca^{2+}$  transient by blocking  $I_{Kur}$ .  $I_{Kur}$  block from 40% to 80% produced long-short-long-short AP and  $Ca^{2+}$  transient alternans at pacing rate of  $\sim 2.3$  Hz to 5 Hz. Further analysis demonstrated that  $I_{Kur}$  block promoted the genesis of AP and  $Ca^{2+}$  transient alternans, via a mechanism of increased AP duration that led to changes of L-type  $Ca^{2+}$  current dynamic, which was a major determinant coupling AP and  $Ca^{2+}$  transient. Our findings suggest that blocking  $I_{Kur}$  may promote the genesis of AP alternans, promote the genesis of AP alternans, indicating a latent pro-arrhythmic effect in normal atria.*

## 1. Introduction

The Kv1.5 channel-mediated, ultra-rapid delayed rectifier  $K^+$  current ( $I_{Kur}$ ) contributes to the early and late repolarization of the action potential (AP), of which function is prominent in atria and negligible in ventricle [1]. Therefore, it is a promising target for class III anti-arrhythmic drugs [2,3], due to the 'atrial-selective' property of the channel. Blocking  $I_{Kur}$  is thought to be a treatment for atrial fibrillation (AF) via reducing

repolarization reserve leading to prolonging action potential duration (APD) or effective refractory period (ERP) with reduced re-entrant tendency [4,5].

In the constant pacing rate, APD prolongation leads to shortening of diastolic interval (DI), resulting in increasing the gradient of APD restitution curves. Some studies have demonstrated that the steep slope of APD restitution is related to the development of APD alternans underlying the voltage-driven mechanism [6-8], even though short-term cardiac memory and calcium cycling dynamics limit predicting APD alternans by the APD restitution slope  $>1$  [9]. However, whether blocking  $I_{Kur}$  induced APD prolongation in normal atria can increase the alternans susceptibility has not yet been investigated. Therefore, this study aimed to investigate the effects of blocking  $I_{Kur}$  on the genesis of repolarization alternans which was associated with arrhythmogenesis.

## 2. Methods

In this study, the canine atrial cell model (the RNC model) developed by Ramirez *et al.* [10] was implemented to examine the effects of blocking  $I_{Kur}$  on genesis of the action potential (AP) alternans. For simulation of  $I_{Kur}$  block, the conductance of  $I_{Kur}$ ,  $g_{Kur}$ , was multiplied by 0.9 to 0.2 responding to blocking  $I_{Kur}$  from 10% to 80%. The RNC model was modified, including reducing the conductance of  $I_{to}$ ,  $I_{Kur}$ ,  $I_{Kr}$ ,  $I_{Ks}$  and  $I_{K1}$  by 10% and increasing the  $I_{NaK}$  by 30%, to maintain the APD relatively stable during the 100 beats and the APD of the 100<sup>th</sup> AP was 184.4 ms at 1Hz in good agreement with experiments [11].

The action potential duration at 90% repolarization (APD<sub>90</sub>) rate dependent curve and restitutions curve were calculated using the dynamic pacing protocol and the standard S1-S2 protocol respectively [12] to analyze the genesis of repolarization alternans under control and  $I_{Kur}$  block conditions. Firstly, the cell model was paced at 1000ms for 100 beats to reach relatively steady state as

initial values for next simulation under control and different  $I_{Kur}$  block conditions. Then, the two protocols were executed. In the dynamic pacing protocol, the cell model was pacing at a fixed cycle length (CL) for 100 beats to reach steady state from 1000 ms to which the APD alternans disappeared. The last two APs were recorded to observe whether there was an alternation with the longer AP and shorter AP. The APDs against different CLs constituted the APD rate dependent curve. In the standard S1-S2 protocol, the cell model was pacing at 1000 ms for 100 beats to reach steady state and then one S2 stimulus was applied after a certain diastolic interval (DI). The resulting APD of S2 stimulus was depending on DI, so that the APD against various DIs constituted the APD restitution curve.

In addition, the changes in the intracellular  $Ca^{2+}$  transient (CaT) amplitude and decay time (calculated as the duration from the peak of the CaT to the time when the intracellular  $Ca^{2+}$  level had been reduced by a factor of e) were evaluated using the two protocols under control and  $I_{Kur}$  block conditions.

### 3. Results

#### 3.1. Effect of blocking $I_{Kur}$ on AP and CaT

Figure 1 shows the effect of blocking  $I_{Kur}$  on the AP morphology, intracellular calcium transient,  $APD_{90}$  and CaT amplitude. The canine atrial  $APD_{90}$  at a pacing rate of 1Hz was prolonged from 184.4 ms in the control condition to 200.4 ms, 205.6 ms, 211.7 ms and 222.4 ms in the 20%, 40%, 60% and 80%  $I_{Kur}$  block condition, and the plateau phase of AP was elevated due to blocking  $I_{Kur}$ . The CaT amplitude was increased from 450.6 nM to 503.7 nM, 545.5 nM, 579.9 nM and 644.8 nM.

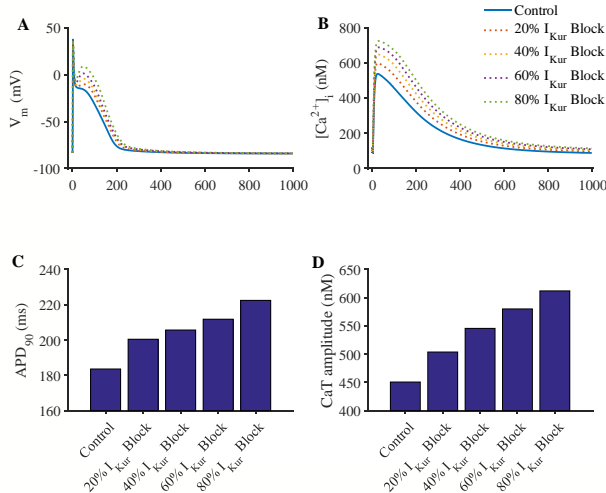


Figure 1. (A) AP morphology, (B) intracellular calcium transient, (C)  $APD_{90}$  and (D) CaT amplitude under control and  $I_{Kur}$  block conditions.

Table 1. The longest CL for the genesis of alternans in  $APD_{90}$ , CaT amplitude ( $CaT_{amp}$ ) and CaT decay time ( $CaT_{DT}$ ).

Blocking $I_{Kur}$	CL ( $APD_{90}$ )	CL ( $CaT_{amp}$ )	CL ( $CaT_{DT}$ )
40%	440 ms	-	440 ms
50%	430 ms	425 ms	435 ms
60%	400 ms	395 ms	405 ms
70%	365 ms	370 ms	375 ms
80%	330 ms	340 ms	340 ms

#### 3.2. APD and CaT alternans under $I_{Kur}$ block conditions

Using the dynamic pacing protocol, the  $APD_{90}$ , CaT amplitude and CaT decay time rate dependent curves were presented in Figure 2 under control and  $I_{Kur}$  block conditions (only shown 20%, 40% and 60%  $I_{Kur}$  block). Genesis of alternans was considered when the beat-to-beat variation  $> 10$  ms in  $APD_{90}$ ,  $> 10$  nM in CaT amplitude or  $> 10$  ms in CaT decay time at the longest CL (details in Table 1). The longest CL for the genesis of alternans was 440 ms in the  $APD_{90}$  and in the CaT decay time when blocking  $I_{Kur}$  by 40%, and the one was 425 ms in the CaT amplitude when blocking  $I_{Kur}$  by 50%. There was no alternans in control condition and in blocking  $I_{Kur}$  by 10% to 30% conditions.  $APD_{90}$  and CaT decay time alternans occurred when blocking  $I_{Kur}$  by 40% to 80%, and CaT amplitude alternans occurred when blocking  $I_{Kur}$  by 50% to 80% (beat-to-beat variation  $< 10$  nM when blocking  $I_{Kur}$  by 40%).

Using the standard S1-S2 protocol, the  $APD_{90}$  restitution curve were presented in Figure 3 under control and  $I_{Kur}$  block conditions (only shown 20%, 40% and 60%  $I_{Kur}$  block). The maximum slope in the control and the 20%  $I_{Kur}$  block conditions were 0.48 and 0.8 which were  $< 1$  and corresponding to no alternans of rate dependent curves in Figure 2. The maximum slope in the 40% and 60%  $I_{Kur}$  block conditions were 1.46 and 2.54 which were  $> 1$  and corresponding to alternans of rate dependent curves in Figure 2 and Table 1. When blocking  $I_{Kur}$  by 40%, the DI with maximum slope was 320 ms with  $APD_{90}$  of 154 ms so that the CL was 474 ms. When blocking  $I_{Kur}$  by 60%, the DI with maximum slope was 234 ms with  $APD_{90}$  of 167ms so that the CL was 401 ms, which was shorter than the one in 40%  $I_{Kur}$  block.

#### 3.3. Mechanism of alternans under $I_{Kur}$ block conditions

Further analysis for the mechanism of alternans under  $I_{Kur}$  block condition was demonstrated in Figure 4 which showed the alternans of  $I_{Kur}$ , AP, intracellular CaT, L-type

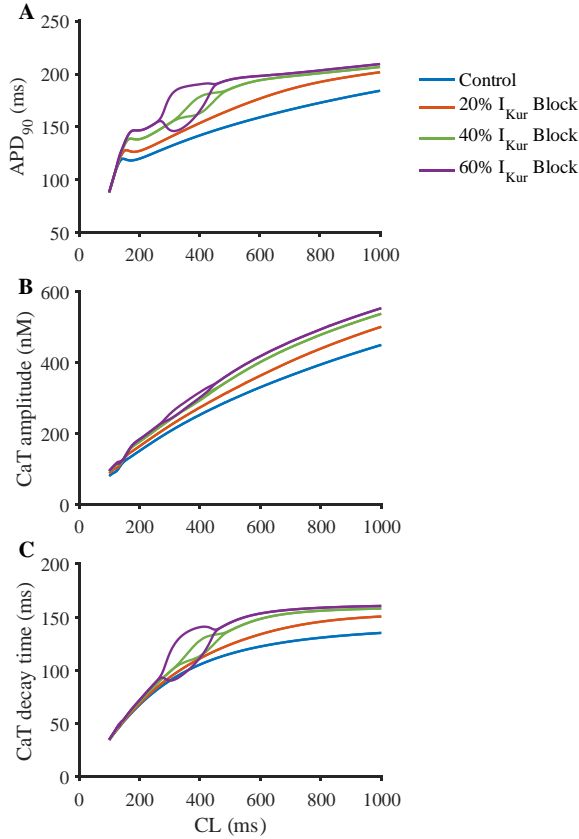


Figure 2. (A) APD<sub>90</sub> and (B) CaT amplitude rate dependent curves under control and  $I_{Kur}$  block conditions.

calcium current ( $I_{CaL}$ ) and its voltage-dependent activation gate ( $d$ ), voltage-dependent inactivation gate ( $f$ ) and calcium-dependent inactivation gate ( $f_{Ca}$ ), and Na-Ca exchange current ( $I_{NCX}$ ) at pacing CL of 400 ms in control and 50%  $I_{Kur}$  block condition. The alternans was in-phase electromechanically representing the long AP with large CaT amplitude and slow rate of decay and the short AP with small CaT amplitude and fast rate of decay (Figure 4B and 4C).

In the long AP, the plateau phase of AP was elevated by blocking  $I_{Kur}$ , which led to extended open time of the  $I_{CaL}$  voltage-dependent activation gate (Figure 4E) resulting in increased transmembrane  $Ca^{2+}$  influx through  $I_{CaL}$ . More  $Ca^{2+}$  influx increased the CaT amplitude and slowed the decay time of  $Ca^{2+}$  transient, so that before the next AP intracellular  $Ca^{2+}$  did not completely recover to diastolic level. Therefore, calcium-dependent inactivation gate of  $I_{CaL}$  was smaller (Figure 4G) before the next AP resulting smaller  $I_{CaL}$  of the next AP (Figure 4D). In addition, due to the long AP, voltage-dependent inactivation gate of  $I_{CaL}$  did not completely recover to the level before this AP (Figure 4F) resulting smaller  $I_{CaL}$  of the next AP. The consequent smaller  $I_{CaL}$  shortened the AP and the plateau phase resulting reduced open time of the  $I_{CaL}$  voltage-dependent activation gate and decreased

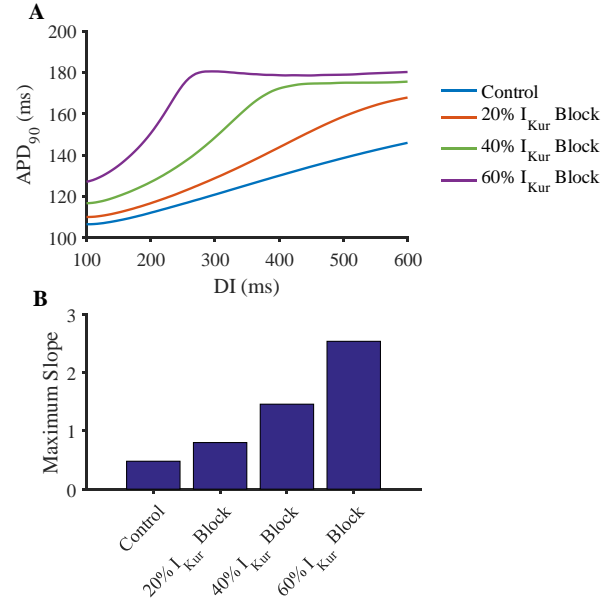


Figure 3. (A) APD<sub>90</sub> restitution curves under control and  $I_{Kur}$  block conditions. (B) The maximum slopes of the APD<sub>90</sub> restitution curves in (A).

transmembrane  $Ca^{2+}$  influx that led to the short AP and small  $Ca^{2+}$  transient. Moreover, the alternans of  $Ca^{2+}$  transient caused alternans of  $I_{NCX}$  which played a significant role in AP repolarisation (Figure 4H).

#### 4. Discussion and conclusion

In this study, the updated canine atrial cell model was used to investigate the effect of blocking  $I_{Kur}$  on the genesis of repolarisation alternans. In this simulation, blocking  $I_{Kur}$  from 40% to 80% produced noticeable long-short-long-short AP and CaT alternans at pacing CL of ~200ms to 440 ms. During these CL, the slope of DI-dependent APD<sub>90</sub> restitution curve was steeper which was related to the genesis of AP alternans. Further analysis for the mechanism of alternans was demonstrated that the effect of  $I_{Kur}$  block on the plateau phase of AP played a significant role in  $I_{CaL}$  which was a major determinant of AP and CaT, consistent with rabbit atrial experimental results that alternation in AP morphology contributed to atrial alternans via  $I_{CaL}$  [13].

In conclusion, this study demonstrates that although prolonging the APD, blocking  $I_{Kur}$  may promote the genesis of AP alternans, indicating a latent pro-arrhythmic effects in normal atria.

#### Acknowledgments

The work is supported by the National Science Foundation of China (NSFC) under Grant Nos. 61572152 (to HZ), 61571165 (to KW), 61601143 (to QL) and

81770328 (to QL), the Science Technology and Innovation Commission of Shenzhen Municipality under Grant Nos. JSJGG20160229125049615 and JCYJ20151029173639477 (to HZ), and China Postdoctoral Science Foundation under Grant Nos. 2015M581448 (to QL).

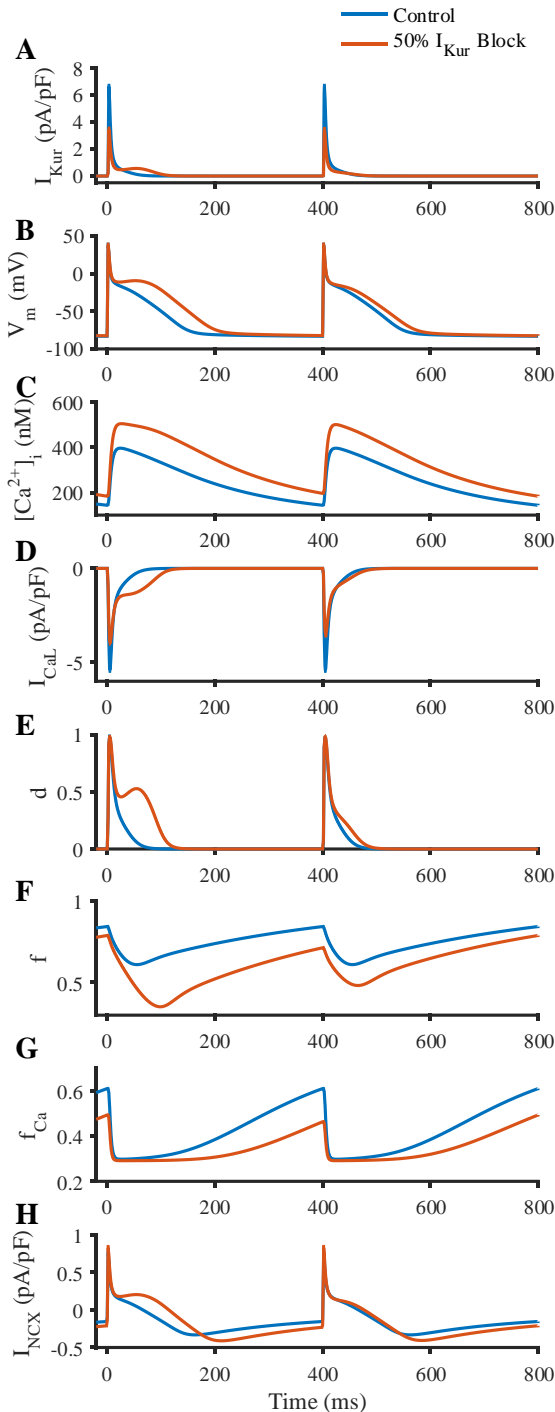


Figure 4. Alternans of (A)  $I_{Kur}$ , (B) AP, (C) intracellular CaT, (D)  $I_{CaL}$ , (E)  $d$ , (F)  $f$ , (G)  $f_{Ca}$ , and (H)  $I_{NCX}$  at pacing CL of 400 ms in control and 50%  $I_{Kur}$  block condition.

## References

- [1] U. Ravens and E. Wettwer, "Ultra-rapid delayed rectifier channels: molecular basis and therapeutic implications," *Cardiovascular research*, vol. 89, no. 4, pp. 776-785, Mar. 2011.
- [2] J. Ford, et al., "The positive frequency-dependent electrophysiological effects of the  $I_{Kur}$  inhibitor XEN-D0103 are desirable for the treatment of atrial fibrillation," *Heart Rhythm*, vol. 13, no. 2, pp. 555-564, Feb. 2016.
- [3] S. Loose, et al., "Effects of  $I_{Kur}$  blocker MK-0448 on human right atrial action potentials from patients in sinus rhythm and in permanent atrial fibrillation," *Front. Pharmacol*, vol. 5, Article.26, Mar. 2014.
- [4] N. Schmitt, M. Grunnet, and S.P. Olesen, "Cardiac potassium channel subtypes: new roles in repolarization and arrhythmia," *Physiol Rev.*, vol. 94, no. 2, pp. 609-653, 2014.
- [5] M. Lei, L. Wu, D.A. Terrar, and C.L.H. Huang, "Modernized classification of cardiac antiarrhythmic drugs," *Circulation*, vol. 138, no.17, pp. 1879-1896, 2018.
- [6] Z. Qu, A. Garfinkel, P.S. Chen, and J/ N. Weiss, "Mechanisms of discordant alternans and induction of reentry in simulated cardiac tissue," *Circulation*, vol. 102, no. 14, pp. 1664-1670, 2000.
- [7] J. I. Goldhaber, et al., "Action potential duration restitution and alternans in rabbit ventricular myocytes: the key role of intracellular calcium cycling," *Circ Res.*, vol. 96, no. 4, pp. 459-466, 2005.
- [8] M.L. Koller, et al., "Altered dynamics of action potential restitution and alternans in humans with structural heart disease," *Circulation*, vol. 112, no. 11, pp. 1542-1548, 2005.
- [9] J.M. Weiss, et al., "From pulsus to pulseless: the saga of cardiac alternans," *Circ Res.*, vol. 98, no. 10, pp. 1244-1253, 2006.
- [10] R.J. Ramirez, S. Nattel, and M. Courtemanche, "Mathematical analysis of canine atrial action potentials: rate, regional factors, and electrical remodeling," *Am J Physiol Heart Circ Physiol*, vol. 279, no. 4, pp. H1767-H1785, 2000.
- [11] Y.H. Yeh, et al., "Calcium-handling abnormalities underlying atrial arrhythmogenesis and contractile dysfunction in dogs with congestive heart failure," *Circ Arrhythmia Electrophysiol.*, vol. 1, no. 2, pp. 93-102, 2008.
- [12] W. Wang, et al., "Mechanistic insight into spontaneous transition from cellular alternans to arrhythmia-A simulation study," *PLoS Comput Biol*, vol. 14, no. 11: e1006594, 2018.
- [13] G. Kanaporis, L. A. Blatter, "Membrane potential determines calcium alternans through modulation of SR  $Ca^{2+}$  load and L-type  $Ca^{2+}$  current," *Journal of Molecular and Cellular Cardiology*, vol. 105, pp. 49-58, 2017.

Address for correspondence:

Henggui Zhang.  
92 West Dazhi Street, Nangang District, Harbin, China  
henggui.zhang@manchester.ac.uk